# Determination of Tumor Necrosis Factor Binding Protein Disulfide Structure: Deviation of the Fourth Domain Structure from the TNFR/NGFR Family Cysteine-Rich Region Signature

Michael D. Jones,[‡] John Hunt,[§] Jennifer L. Liu,[‡] Scott D. Patterson,[‡] Tadahiko Kohno,[§] and Hsieng S. Lu*[,‡]

*Department of Protein Structure, Amgen Inc., Amgen Center, Thousand Oaks, California 91320, and Amgen Inc., Boulder, Colorado*

*Received July 14, 1997; Revised Manuscript Received September 16, 1997*[⊗]

ABSTRACT: Tumor necrosis factor binding protein is a soluble molecule derived from the extracellular domain of the 55 kDa human tumor necrosis factor receptor, which can block the biological function of tumor necrosis factor by binding to the growth factor. This cysteine-rich molecule is subdivided into four domains, each containing six conserved cysteines that form three intrachain disulfide linkages known as the tumor necrosis factor receptor/nerve growth factor receptor family cysteine-rich region signature structure. In an effort to elucidate the molecular integrity of the molecule, we performed detailed analysis and searched for strategies to elucidate the complete disulfide structure of the *E. coli*-derived tumor necrosis factor binding protein and to determine the disulfide arrangement in the fourth domain of Chinese hamster ovary cell-derived molecule. The methods employed included various proteolytic digestions, peptide mapping, partial reduction, and assignment of disulfides by N-terminal sequencing and matrix-assisted laser desorption ionization mass spectrometry with post-source decay. The first three domains of the molecule were confirmed to have disulfide structures identical to the cysteine-rich region signature structure found in the above-mentioned receptor superfamily. The fourth domain has a different structure from the first three domains where the last four cysteines form two disulfide bonds in opposite positions.

Tumor necrosis factor-α (TNFα)[1] and its closely related molecule lymphotoxin/TNF$\beta$ are now recognized as powerful cytokines involved in immune and proinflammatory responses. These cytokines exhibit a number of important cellular functions, including cytotoxicity, antiviral activity, apoptosis, and immunoregulatory activity (*1*). These biological effects are signaled through two TNF receptors: TNF-R1 of 55 kDa and TNF-R2 of 75 kDa, respectively (*2*−*4*). The receptors belong to the cysteine-rich low-affinity nerve growth factor receptor (NGF-R) superfamily which includes FAS, CD40, OX40, CD27, and several viral proteins (*5*) and are structurally distinct from the cysteine knot class of proteins (*6*). Across the family the pattern of cysteines was found to be highly similar among the extracellular domains. Recently a soluble form of TNF-R1 (or TNFbp) containing only the extracellular domain of the receptor has been identified in serum and confirmed to down-regulate TNF functions by competing with the receptor for TNF binding (*7*). Preclinical studies indicated that the soluble receptor or TNFbp could function as a therapeutic to inhibit inflammatory and immune responses in animals (*8*, *9*).

TNFbp consists of four subdomains, each of which contains six conserved cysteines and has similarity in the pattern of cysteines, suggesting a similarity in their intramolecular disulfide pairing (*5*). The crystal structures of the TNF-R1 extracellular domain in both the unliganded and the TNF-bound state have been elucidated at pH 7.5 (*10*, *11*). In these structures, the fourth domain was partly disordered, and the disulfide connectivity of all but the last two disulfides was determined. Recently the structure has also been solved at low pH under high salt conditions (*12*). One of the packing environments generated a structure which had an ordered fourth domain near the C-terminus. The disulfide connectivity in the fourth domain was observed to be different from what was observed in the other subdomains.

We have engineered a recombinant form of TNFbp to be expressed in a bacterial or mammalian expression system. In bacterial expression, the originally reduced and unfolded TNFbp is oxidized and refolded in the presence of cysteine to allow correct pairing of all disulfide bonds. With a complex disulfide structure like TNFbp, it is difficult to rule out the possibility that disulfide-mispaired species can be copurified with the biologically active form. While X-ray crystallographic analyses provided important insight about the TNFbp molecular structure and arrangement of disulfide bonds, there have been no data to confirm that the engineered protein contains all correctly paired disulfides in solution and at physiological pH. In this report, we have elucidated the complete disulfide structure of *E. coli*-derived TNFbp and the last two disulfide pairs of the fourth domain from CHO cell-derived TNFbp using several different chemical strategies. The methods included various proteolytic diges-

* Address correspondence to this author at Amgen Inc., M/S 14-2-E, Amgen Center, Thousand Oaks, CA 91320-1789. Telephone: 805-447-3092. Fax: 805-499-7464.

[‡] Amgen Center, Thousand Oaks, CA.

[§] Amgen Inc., Boulder, CO.

[⊗] Abstract published in *Advance ACS Abstracts,* November 1, 1997.

[1] Abbreviations: TNFbp, tumor necrosis factor binding protein; CHO, Chinese hamster ovary; DTT, dithiothreitol; TFA, trifluoroacetic acid; IAA, iodoacetic acid; RP-HPLC, reverse-phase high-performance liquid chromatography; SDS, sodium dodecyl sulfate; 4HCCA, α-cyano-4-hydroxycinnamic acid; DHB, 2,5-dihydroxybenzoic acid; MS, mass spectrometry; MALDI-MS, matrix-assisted laser desorption ionization MS; CR-, curve field reflectron-; PSD, post-source decay; CID, collision-induced dissociation; LC-MS, liquid chromatography in conjunction with MS analysis.

S0006-2960(97)01696-6 CCC: $14.00 

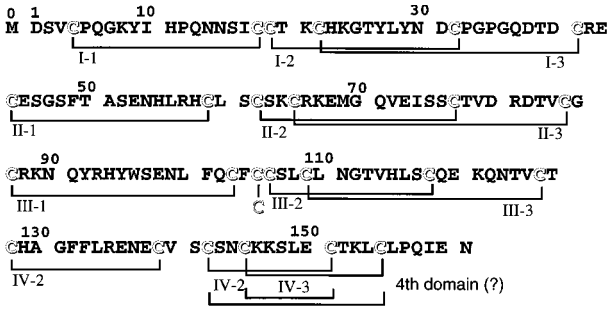


FIGURE 1: Amino acid sequence and proposed disulfide arrangement of bacterially derived recombinant human Cys105 TNFbp. An extra Met is present at the N-terminus. All proposed disulfide bonds are indicated. The last two pairs in the fourth domain are unclear, but X-ray analysis at low pH revealed an arrangement of these two disulfides different from the other three domains.

tions, peptide mapping, partial reduction, N-terminal sequencing, and matrix-assisted laser desorption ionization mass spectrometry with post-source decay (PSD). The elucidation of the complete disulfide structure of TNFbp confirmed that the engineered protein does refold properly and that the last two disulfide pairs in the fourth domain structure are different from what were seen in the first three domains as in the pH 3.5 crystal structure.

## MATERIALS AND METHODS

*Materials.* Gene encoding human TNFbp containing an initiating methionine codon followed by codons for amino acids 1−161 was constructed (*13*). Amino acid Ser at position 105 has been mutated to cysteine by site-directed mutagenesis to generate recombinant Cys105 TNFbp. Recombinant Cys105 TNFbp was expressed in *E. coli* and isolated according to methods described previously (*14*). The expressed protein accumulated in the inclusion bodies was solubilized in guanidine hydrochloride and then reduced by dithiothreitol under alkaline pH (pH 8.5). Mixed thiols were formed by treating the reduced protein with oxidized glutathione; and following dilution, the sample was allowed to refold in the presence of cysteine (*15*). Refolded Cys105 TNFbp was then purified by an TNF-α-affinity column and conventional column chromatography as described. The recombinant molecule contains 162 amino acids including an N-terminal initiator methionine. Figure 1 illustrates the amino acid sequence and the proposed disulfide arrangement of recombinant human Cys105 TNFbp. Note that the proposed structure contains a similar disulfide pattern in each domain, with a possible exception that the last two disulfides in the fourth domain are different based on crystallographic analysis. Recombinant Chinese hamster ovary cell-derived TNFbp (CHO-TNFbp) was also expressed according to a previously reported procedure (*16*) and purified following various chromatographic procedures.[2] In comparison with *E. coli*-derived Cys105 TNFbp (Figure 1), the recombinant TNFbp produced in CHO cells is a longer molecule (182 amino acids) with an additional 11 amino acids at the N-terminus (sequence: L-V-P-H-L-G-D-R-E-K-R-) and 10 amino acids at the C-terminus (sequence: -V-K-G-T-E-D-S-G-T-T) and contains both Asn-linked and O-linked carbohydrates (T. Eris et al., unpublished data).

[2] Mike Kelley et al., unpublished data.

Trypsin (sequencing grade), thermolysin, and tris(2-carboxyethyl)phosphine (TCEP) were purchased from Boehringer Mannheim (Indianapolis, IN). Iodoacetic acid was purchased from Sigma. HPLC solvents and water were purchased from Burdick and Jackson (Mcgaw Park, IL). Sequencing reagents and solvents were supplied by Perkin Elmer-Applied Biosystems Division (Foster City, CA) and Hewlett Packard (Palo Alto, CA). Pre-made matrix solution, 4HCCA (α-cyano-4-hydroxycinnamic acid; 33 mM in acetonitrile/methanol/water, 5:3:2 v/v), and DHB (2,5-dihydroxybenzoic acid; 100 mM in 50% methanolic water) were purchased from Hewlett Packard. All other reagents were of the highest quality available.

*Chromatographic Peptide Mapping.* Peptide mapping of peptide mixtures generated from protease digestion or partial reduction of disulfide-linked peptides was performed on a Hewlett-Packard 1090M liquid chromatograph (Palo Alto, CA) using different types of reverse phase columns (i.e., Vydac 5 $\mu$m C4 column, 4.6 × 250 mm; 5 $\mu$m C18 column, 4.6 × 250 mm; or 5 $\mu$m C4 column, 2.1 × 250 mm; The Separations Group, Hesparia, CA). The columns were equilibrated with 97% mobile phase A (0.1% TFA) and 3% mobile phase B (0.1 % TFA in 90% acetonitrile) at a flow rate of 0.7 mL/min for the 4.6 mm i.d. columns or at 0.2 mL/min for the 2.1 mm columns. Peptide mixtures were injected onto the column and eluted with the following elution program for various types of columns as described above: an isocratic elution at 3% mobile phase B for 5 min followed by a series of linear gradients, i.e., 23% B in 80 min, 40% B in 10 min, and 90% B in 5 min.

*Proteolytic Digestions of Cys105 TNFbp.* A 1 mg/mL solution of Cys105 TNFbp in 0.1 M Tris-HCl containing 1 mM $CaCl_2$ (pH 7.0) was digested with trypsin or thermolysin (both at an enzyme-to-substrate ratio of 1:25) for 18 h at 37 °C. Digests were then injected onto the RP-HPLC column for peptide isolation and identification or stored frozen at −20 °C.

*Thermolysin Digest of Tryptic Peptides.* Peptides were collected and pooled from three separate RP-HPLC peptide maps derived from 14 nmol of peptide digest. The combined fractions (approximately 10 nmol) were reconstituted in 200 $\mu$L of digestion buffer as described above. Some peptide fractions were redigested with trypsin as described above. The remaining samples were then digested with thermolysin for 18 h at 37 °C. Digests were immediately subjected to HPLC peptide mapping as described.

*Proteolytic Digestions of CHO Cell-Derived TNFbp.* Thermolysin digestion for CHO cell-derived TNFbp was carried out in 100 mM sodium phosphate containing 10 mM $CaCl_2$ (pH 6.0) at 37 °C for 18 h, with an enzyme-to-substrate ratio of 1:20. Secondary trypsin digestion of the isolated peptides was done using a Porozyme immobilized trypsin column (PerSeptive Biosystems, Framingham, MA) in 50 mM Tris-HCl (pH 8.2) at 50 $\mu$L/min for 5 min at 37 °C. Peptides were separated using a microbore C18 column (1.0 mm × 250 mm; Vydac) with a linear gradient of 1% mobile phase B/min. Mobile phase A was $H_2O$/acetonitrile/TFA (98:2:0.05, v/v), while mobile phase B was at a ratio of 10:90:0.04.

*Partial Reduction of Peptides by TCEP.* TCEP partial reduction experiments (*17*) were performed as described below. A sample vial containing approximately 250 pmol of the peptide fraction in 50 $\mu$L of 0.1% TFA and 20%

acetonitrile was added to 50 $\mu$L of TCEP solution (20 mM) in 0.02 M sodium citrate, pH 3.0, and incubated for 1−10 min at room temperature. Alkylation of TCEP-reduced peptides was performed by incubating the sample with 50 $\mu$L of 1 M iodoacetic acid in 1.0 M Tris, pH 8.0, for 2 min at 25 °C. The derivatized sample was immediately injected onto a RP-HPLC column for analysis.

*Sequence Analysis.* Sequence analysis of peptides was performed on automated protein sequencers (Applied Biosystems, Model 477A or 470, and Hewlett Packard, Model HPG1000A) using procedures as described previously (*18*). PTH-amino acid separation by narrowbore reverse-phase HPLC was performed according to Vendors' recommendation. PTH-cystine detection and quantitation at specific sequencing cycles were applied to identify disulfide linkage(s) between individual peptide sequences in several disulfide-linked peptide fractions (*18*, *19*).

*Mass Spectrometry.* Matrix-assisted laser desorption ionization mass spectrometry (MALDI-MS) of *E. coli*-derived TNFbp peptides was performed on a Kompact MALDI IV mass spectrometer (Kratos Analytical, Ramsey, NJ) equipped with a curved field reflectron and a precursor ion gate (*20*). Spectra were obtained in either the linear mode, at an acceleration voltage of 20 kV, or the reflector mode, with the linear voltage at 20 kV and the ion mirror set at 21 kV. The MALDI IV laser power can be adjusted from a relative scale (from 0 to 180) set by the manufacturer, in which the threshold of detection ranged from 45 to 65 in the linear mode and from 85 to 105 in the reflectron mode for post-source decay. Aliquots of sample (0.7 $\mu$L) and matrix solution (0.4 $\mu$L) were properly mixed and spotted onto the probe slide. Following an air-dry step, the sample was ready for analysis. In the linear mode (referred to as MALDI-MS), some prompt fragmentation of disulfide bonds in disulfide-linked peptide samples occurs at low laser power, but it can be enhanced by increasing the laser power during analysis. In the reflectron mode (referred to as CR-MALDI-PSD), specific parent ions can be selected by the precursor ion gate and fragmented at a higher laser power (see above). For linear mode analysis, the instrument was calibrated externally with oxidized insulin B-chain (*m*/*z* 3497) and a HCCA matrix ion (*m*/*z* 172) in a least-squares regression analysis with the Kratos Kompact software. In a reflectron mode analysis, the mass spectrometer was calibrated using a calibrant described by Cordero et al. (*21*). Briefly the peptide Pro14Arg containing 14 proline residues and a C-terminal arginine (average protonated mass of 1534.8) was fragmented, and the obtained fragment ions were calibrated based on the expected fragment ion masses. An elliptical equation was generated and can be used later to automatically calibrate the fragmented ions after identification of the parent ion. For post-source decay analysis of CHO cell-derived TNFbp peptides, a Voyager-DE-RP MALDI analyzer (PerSeptive Biosystems) was used. The instrument was equipped with a nitrogen laser ($\lambda = 337$ nm) and fitted with a collision cell for CID/PSD. The mass spectrometric analysis was operated in the linear mode with an accelerating voltage of 20 kV (referred to as MALDI-MS). The laser power was set at 2600, and data collection was averaged over 64 scans. Prompt fragmentation of disulfide-linked peptides was not performed using this equipment; however, post-source decay was accomplished with an accelerating voltage of 20 kV using room air as the collision gas at a pressure of 1.00 e-06 and a laser setting of 1975 V (referred to as CID-MALDI-PSD).

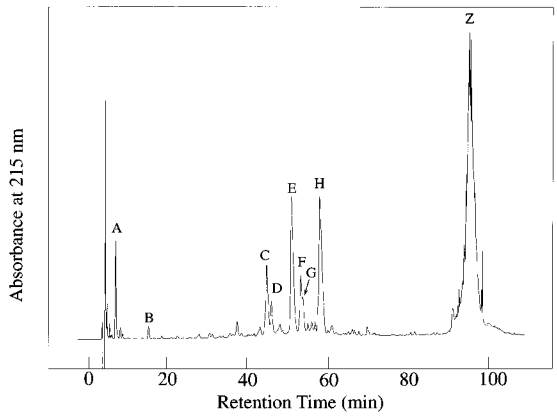


FIGURE 2: Reverse-phase HPLC peptide map of a tryptic digest derived from 10 nmol of Cys105 TNFbp using a narrowbore C4 column (2.1 × 250 mm).

Electrospray ionization mass spectrometry of peptide samples was performed on a Sciex API-I00 (Thornhill, Ontario, Canada) by direct infusion of peptide solution at a flow rate of 2−5 $\mu$L/min. LC-MS was performed by splitting the outlet line with 20% going directly to the mass spectrometer. The scan range on the mass spectrometer was set from *m*/*z* 300 to 1800, with an orifice voltage of 75 V, step size of 0.15 Da, and a dwell of 0.5 ms. The chromatographic conditions for LC/MS were the same as described above.

Electrospray ionization quadrupole ion trap mass spectrometry (ESI-QIT-MS) was performed on a Finnigan MAT ion trap mass spectrometer (San Jose, CA) according to procedures described (*22*, *23*). Samples collected in RP-HPLC mobile phase were analyzed directly or concentrated to dryness in a polypropylene microcentrifuge tube and reconstituted in 15% acetonitrile in 0.1% TFA. Analysis was performed by flow injection at a flow rate of 20 $\mu$L/min. Mass spectra were collected in the positive ion mode scanning between mass ranges of 150 and 1500 Da. Individual ions were selected for fragmentation in the ion trap and fragmented with a relative collision energy of 35%.

## RESULTS AND DISCUSSION

*Tryptic Digestion and Peptide Mapping.* Figure 2 illustrates a reverse phase HPLC peptide map of the Cys105 TNFbp tryptic digest using a narrowbore C4 column. Nine major peaks, designated from peptide fractions A−Z, were recovered. Results of amino acid sequence determination of isolated peptides by automated sequencing and measurement of molecular masses by mass spectrometry are listed in Table 1. The analyses indicated that both fractions A (sequence 90−93, N-Q-Y-R) and B (sequence 9−15, Y-I-H-P-Q-N-N) are non-disulfide-linked peptides while the remaining peptide peaks contain multiple peptide sequences held together by disulfide bonds. As seen in Table 1, tryptic digestion of Cys105 TNFbp generates complex disulfide-linked tryptic peptides. A complete and specific tryptic cleavage of Cys105 TNFbp at the expected cleavage sites near Lys and Arg is expected to generate three major disulfide-containing peptide fractions. Detailed sequencing and mass spectrometic analysis confirm that fractions E, H, and Z represent these three peptide species. The cleavage

Table 1: Assignment of Cys105 TNFbp Tryptic Peptides

| peptide fractions | assigned positions | sequence[a] | average mass[b] (Da) calcd | obsd |
|---|---|---|---|---|
| A | 90−93 | N-Q-Y-R | 580.6 | 580.2 |
| B | 9−15 | Y-I-H-P-Q-N-N | 886.0 | 885.3 |
| C | 0−8 | M-D-S-V-C-P-Q-G-K | | |
| | 16−21 | S-I-C-C-T-K | | |
| | 25−42 | G-T-Y-L-Y-N-D-C-P-G-P-G-Q-D-T-D-C-R | | |
| | 22−24 | C-H-K | 3973.5 | 3973.5 |
| D | 0−8 | M-D-S-V-C-P-Q-G-K | | |
| | 9−21 | Y-I-H-P-Q-N-N-S-I-C-C-T-K | | |
| | 28−42 | L-Y-N-D-C-P-G-P-G-Q-D-T-D-C-R | | |
| | 22−24 | C-H-K | 4519.2 | 4519.4 |
| E | 0−8 | M-D-S-V-C-P-Q-G-K | | |
| | 9−21 | Y-I-H-P-Q-N-N-S-I-C-C-T-K | | |
| | 25−42 | G-T-Y-L-Y-N-D-C-P-G-P-G-Q-D-T-D-C-R | | |
| | 22−24 | C-H-K | 4841.5 | 4840.4 |
| F | 0−8 | M-D-S-V-C-P-Q-G-K | | |
| | 9−24 | Y-I-H-P-Q-N-N-S-I-C-C-T-K-C-H-K | | |
| | 25−42 | G-T-Y-L-Y-N-D-C-P-G-P-G-Q-D-T-D-C-R | 4824.4 | 4824.1 |
| G | 43−55 | E-C-E-S-G-S-F-T-A-S-E-N-H | | |
| | 58−64 | H-C-L-S-C-S-K | | |
| | 68−81 | E-M-G-Q-V-E-I-S-S-C-T-V-D-R | 3724.9 | 3725.5 |
| H | 43−57 | E-C-E-S-G-S-F-T-A-S-E-N-H-L-R | | |
| | 58−64 | H-C-L-S-C-S-K | | |
| | 68−81 | E-M-G-Q-V-E-I-S-S-C-T-V-D-R | 3994.4 | 3993.8 |
| Z | 65−66(67) | C-R-(K) | | |
| | 82−88 | D-T-V-C-G-C-R | | |
| | 94−121 | H-Y-W-S-E-N-L-F-Q-C-F-C-C-S-L-C-L-N-G-T-V-H-L-S-C-Q-E-K | | |
| | 122−135 | Q-N-T-V-C-T-C-H-A-G-F-F-L-R | | |
| | 136−146 | E-N-E-C-V-S-C-S-N-C-K | | |
| | 148−153 | S-L-E-C-T-K | | |
| | 154−161 | L-C-L-P-Q-I-E-N | | |
| | | C | 8851.1 (8979.7) | 8853.1 (8980.0) |

[a] Single-letter standard amino acid codes were used. [b] Masses were determined by MALDI-MS in the linear mode or ESI-MS (see Materials and Methods for details).

of the Arg-42 bond separates the N-terminal domain I structure from the remaining disulfide structures. Sequence and mass spectrometric analyses (see Figure 2 and Table 1) indicate that fractions C, D, E, and F are all domain I disulfide-containing peptides. Fraction E represents the expected major fraction derived from specific cleavage of the protein at Lys9, Lys21, Lys24, and Arg42, while fractions C and D are products of fraction E derived from nonspecific tryptic cleavage at Asn15 and Tyr27, respectively. Fraction F containing three sequences also differs from fraction E, in that there is no cleavage at Lys21 as confirmed by both sequence analysis and mass measurement (Table 1). Fraction H represents the product from specific cleavage of Cys105 TNFbp at Arg42, Arg57, Lys64, Arg66, and Arg81. This fraction contains the putative first and second disulfide bonds in domain II. Nonspecific cleavage of fraction H at His55 generates fraction G (see Figure 1 and Table 2). Fraction Z is the largest disulfide-linked peptide containing the disulfide bonds from domains III and IV and the last disulfide bond of domain II. Mass determination and N-terminal sequence analysis predicted that this fraction contains a multiple disulfide-linked peptide cluster covering structures in the third and fourth domain and one disulfide pair in the second domain.

Prompt disulfide fragmentation of disulfide-linked peptides during MALDI analysis has been reported in a linear positive ion mode (*24*, *25*). Laser power-induced in-source cleavage of a disulfide bond generates a pair of reduced peptides from those originally held together as a disulfide-linked peptide, allowing an unambiguous assignment of disulfide bridges. This technique also proved to be useful in the verification of Cys105 TNFbp tryptic peptide fractions containing multiple sequences held together by disulfide bonds. Figure 3 shows a mass spectrum generated by prompt fragmentation of fraction E during MALDI analysis. Electrospray or ion-trap mass spectrometric analysis produces only a single mass of 4842.0 Da for this peptide (Table 1). However, following prompt fragmentation in a MALDI analysis, in addition to the parent mass, additional masses at lower mass ranges were detected. These ions include four reduced species (masses of 386.5, 964.9, 1519.1, and 1975 Da) as well as ions with every other partially reduced species. A total of five partially reduced species were generated from fraction E. The detection of these ions reduces the possible disulfide linkages to four, instead of eight, to connect these four Cys105 TNFbp tryptic peptides together. Therefore, despite that MALDI prompt fragmentation experiments are not sufficient for assigning disulfide bonds in peptides containing more than two disulfide bonds, it significantly reduces the number of possible disulfide arrangement. The method appears to provide accurate mass measurement to determine which peptides constitutes an intact disulfide-linked peptide and further validate the classical sequencing data. Results from both prompt fragmentation coupled with N-terminal sequence

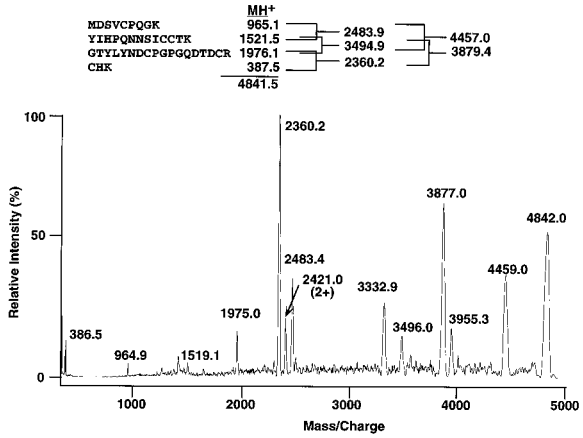


FIGURE 3: MALDI prompt fragmentation of tryptic peptide E (see Figure 2). The unfragmented molecular ion of this peptide is 4842.0 Da (doubly charged ion = 2421.0 Da). The predicted masses for each of the four reduced peptides as well as those partially cleaved at various disulfide bonds are indicated. Two unknown ions were also observed at 3332.9 and 3955.3 Da.

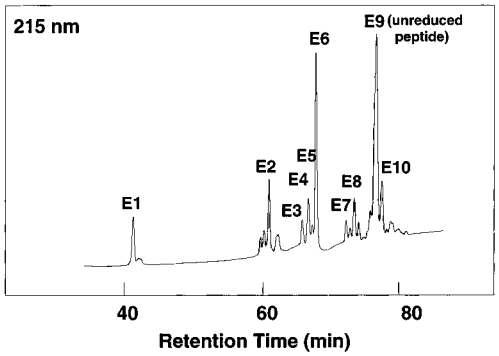


FIGURE 4: Reverse-phase HPLC analysis of tryptic peptide E following TCEP partial reduction (see Materials and Methods for details). Peptide E9 is the intact peptide not reduced by TCEP. Few small peaks without peak numbering cannot be identified by N-terminal sequence analysis.

analysis were therefore useful in identifying all isolated disulfide-linked peptide fractions. Peptide fraction Z is the only sample that does not generate good prompt fragmentation data possibly due to its larger molecular size.

Since tryptic digestion of Cys105 TNFbp was unable to release any peptides that contain a single disulfide bond, no disulfide linkages could be assigned directly from the tryptic peptide fractions shown in Figure 1. Further digestion and characterization of some of these isolated peptide fractions using various strategies are therefore employed to elucidate the assignment of 13 disulfide bonds in the Cys105 TNFbp molecule.

*Partial Reduction and Assignment of the Disulfide Structure of Tryptic Peptide E (Domain I Disulfide-Linked Peptide).* As described above, trypic peptide E fraction contains domain I tryptic peptides linked by three disulfide bonds. This peptide fraction was subjected to TCEP partial reduction followed by carboxymethylation and then subjected to reverse phase HPLC peptide mapping. Figure 4 shows the peptide map of peptide E fraction after partial reduction and alkylation. The use of the strong reducing agent TCEP which reduces disulfides at low pH within a short incubation time was found to minimize both thiol−disulfide exchange and disulfide rearrangement in the partially reduced peptides (*17*). The major peptide sequences as well as the modified cysteine residues [in the form of (carboxymethyl)cysteine] can be identified by N-terminal sequencing. Table 2 summarizes the results. Peptides E1, E2, and E6 are peptides that have been completely reduced and alkylated, while peptides E4, E5, and E10 are partially reduced and alkylated peptides. Methionine carboxymethylation of peptide E10, a common side reaction seen under higher alkylation concentrations (*26*), resulted in the generation of peptide E8. Peptide E9 is the original nonmodified peptide. Characterization of the partially reduced peptides and identification of a paired cystine in the sequences of partially reduced but still disulfide-linked peptides allow the elucidation of the disulfide structure in peptide E. E4 is comprised of two tryptic peptides (sequences 25−42 and 22−24) linked together by a single disulfide bond, Cys22−Cys41, where Cys32 has been reduced and alkylated. Likewise, E5 also contains two tryptic peptides (sequences 0−8 and 9−21) connected together by a single disulfide bridge, Cys4−Cys18, where the Cys19 is identified to be reduced and alkylated. By elimination, the two reduced and alkylated residues, Cys19 and Cys32, should form another disulfide bond. Further evidence for the assignment is provided by the analysis of peptide E10. This peptide contains three peptides linked by two disulfide bonds and Cys41 is reduced and alkylated. Since the sequence C-H-K at positions 22−24 is missing in the peptide due to reduction and alkylation of Cys41, peptide E10 is clearly derived from cleavage of the Cys22−Cys41 bond by partial reduction of peptide E. The above assignment is also consistent with one of the four possibilities predicted from the prompt fragmentation data (see Figure 3). Therefore, the three disulfide bonds for the domain I peptide fractions C, D, and E can be assigned by the partial reduction strategy as described and proved to have the following linkages: Cys4−Cys18, Cys19−Cys32, and Cys22−Cys41.

*Analysis of Tryptic Peptide Fractions G and H.* These two peptide fractions contain the first two disulfide bonds in domain II (see Figure 1 and Table 1). As a single molecular ion mass matching fractions G and H can be determined (Table 1), the detected three peptide sequences must be held together by two disulfide bonds; and there are only two possibilities for the pairing, indicating that Cys44 in the first peptide (sequence 43−55 or 43−57) and Cys77 in the second peptide (sequence 68−81) must link to Cys59 and Cys62 in the third peptide (sequence 58−64). Reduction of the fractions by TCEP results in complete reduction of all peptides, yielding no merit for the assignment. MALDI prompt fragmentation of the peptide clearly confirmed that the two single Cys-containing peptides are disulfide-linked to the peptide containing two Cys residues (data not shown). Disulfide assignment can not be made by post-source decay experiments during MALDI analysis of the sample (see below for detail) due to limited fragmentation (i.e., only cleavage of a C-terminal Arg and the disulfide bonds). However, in carefully examining the N-terminal sequence data as listed in Table 3, the recovery of PTH-cystine in addition to PTH-methionine is significant at the second sequencing cycle during automated Edman degradation. The detection of a cystine residue at this sequencing step clearly indicates that Cys44 and Cys59 form a disulfide bond (for reference, see *18*, *19*). PTH-cystine derived from the Cys62−Cys77 bond was also at the 10th sequencing cycle but with slightly lower yield (Table 3).

Table 2: Assignment of Sequences of Peptides Derived from TCEP Partial Reduction of Tryptic Peptide Fraction E

| peptide fractions | assigned positions | sequence[a] | assignment of disulfide bond(s) |
|---|---|---|---|
| E1 | 0−8 | M-D-S-V-cmC-P-Q-G-K | reduced peptide |
| E2 | 9−21 | Y-I-H-P-Q-N-N-S-I-cmC-cmC-T-K | reduced peptide |
| E4 | 25−42 | G-T-Y-L-Y-N-D-cmC-P-G-P-G-Q-D-T-D-**C**-R | Cys22 to Cys41 |
| | 22−24 | **C**-H-K | |
| E5 | 0−8 | M-D-S-V-**C**-P-Q-G-K | Cys4 to Cys18 |
| | 9−21 | Y-I-H-P-Q-N-N-S-I-**C**-cmC-T-K | |
| E6 | 25−42 | G-T-Y-L-Y-N-D-cmC-P-G-P-G-Q-D-T-D-cmC-R | Reduced peptide |
| E7 | 0−8 | cmM-D-S-V-**C**-P-Q-G-K | |
| | 9−21 | Y-I-H-P-Q-N-N-S-I-**C**-cmC-T-K | Cys4 to Cys18 |
| E8 | 0−8 | cmM-D-S-V-C-P-Q-G-K | |
| | 9−21 | Y-I-H-P-Q-N-N-S-I-C-C-T-K | |
| | 25−42 | G-T-Y-L-Y-N-D-C-P-G-P-G-Q-D-T-D-C-R | |
| | 22−24 | C-H-K | |
| E9 | 0−8 | M-D-S-V-C-P-Q-G-K | |
| | 9−21 | Y-I-H-P-Q-N-N-S-I-C-C-T-K | |
| | 25−42 | G-T-Y-L-Y-N-D-C-P-G-P-G-Q-D-T-D-C-R | |
| | 22−24 | C-H-K | nonreduced peptide E |
| E10 | 0−8 | M-D-S-V-**C**-P-Q-G-K | |
| | 9−21 | Y-I-H-P-Q-N-N-S-I-**C**-**C**-T-K | |
| | 25−42 | G-T-Y-L-Y-N-D-**C**-P-G-P-G-Q-D-T-D-cmC-R | Cys4 to Cys18<br>Cys19 to Cys32 |

[a] Single-letter standard amino acid codes were used. cmC: (carboxymethyl)cysteine.

Table 3. Sequence Analyses of Peptides H, H2, Z8, and Z11

| peptide H | | peptide H2 | | peptide Z8 | | peptide Z10 | |
|---|---|---|---|---|---|---|---|
| cycle | sequence | cycle | sequence | cycle | sequence | cycle | sequence |
| 1 | Glu (1907)[a] | 1 | Ile (35.1) | 1 | Val (123.3) | 1 | Phe (25.6) |
| | His (750) | | Leu (45.5) | | Glu (76.1) | | Val (34.6) |
| 2 | cystine[b] (125) | 2 | Ser (32.2) | | Leu (94.2) | 2 | Gln (27.2) |
| | Met (786) | 3 | Ser (20.1) | 2 | Asn (99.8) | | Arg (5.6) |
| 3 | Glu (750) | 4 | cystine (7.1) | | cystine (46.7) | | cystine (7.0) |
| | Leu (599) | 5 | Thr (10) | 3 | Thr (42.1) | 3 | Gly (27.2) |
| | Gly (555) | 6 | − | | Glu (64.2) | 4 | cystine (2.2) |
| 4 | Ser (371) | 7 | − | 4 | cystine (12.0) | 5 | Arg (2.5) |
| | Gln (653) | | | 5 | − | 6 | − |
| 5 | Gly (398) | | | 6 | − | 7 | − |
| | Val (477) | | | | | | |
| 6 | Ser (362) | | | | | | |
| | Glu (650) | | | | | | |
| 7 | Phe (556) | | | | | | |
| | Lys (424) | | | | | | |
| | Ile (187) | | | | | | |
| 8 | Thr (266) | | | | | | |
| | Ser (175) | | | | | | |
| 9 | Ala (446) | | | | | | |
| | Ser (197) | | | | | | |
| 10 | Ser (163) | | | | | | |
| | cystine (45) | | | | | | |
| 11 | Glu (350) | | | | | | |
| | Thr (197) | | | | | | |
| 12 | Asn (347) | | | | | | |
| | Val (225) | | | | | | |
| 13 | His (136) | | | | | | |
| | Asp (250) | | | | | | |
| 14 | Leu (240) | | | | | | |
| | Arg (144) | | | | | | |
| 15 | Arg (339) | | | | | | |

[a] The number in parentheses indicates the recovery yield (in picomoles) of PTH-amino acids at each sequencing cycle. [b] Recovery of PTH-cystine was calculated according to previously reported procedures (*19*).

Peptide fraction H was further subjected to thermolysin digestion and the digest analyzed by LC-MS analysis using a quadrupole ion-trap mass spectrometer. Shown in Figure 5A is the LC tracing detected at 215 nm. Two peptide peaks, H1 and H2, were recovered. Peptide fraction H1 had a molecular mass of 805.2 Da and a sequence of E-M-G-Q-V-E-I by direct N-terminal sequence determination, and peptide H2 contains two peptides that are disulfide-linked, with a mass of 829.1 Da ($MH^+$) (Figure 5, panel B) and peptide sequences of I-S-S-C-T (sequence 74−78) and L-S-C

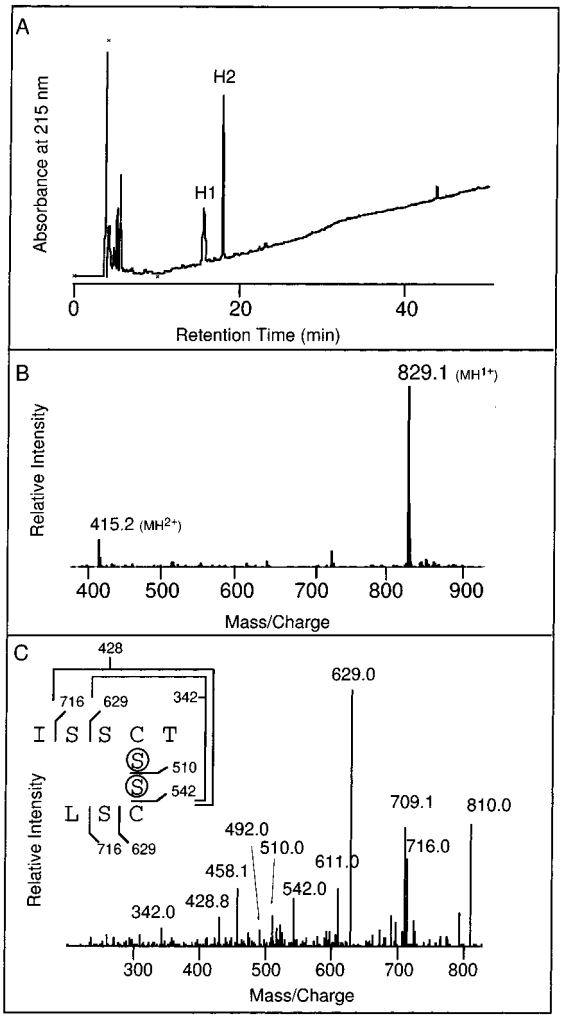


FIGURE 5: Quadrupole ion-trap LC-MS analysis of tryptic peptide H following thermolysin digestion. A micro LC chromatographic trace detected at 215 nm is shown in panel A. The MS scan for peptide H2 is shown in panel B. The tandem mass spectrometric analysis of the peptide is shown in panel C for verification of the disulfide bond. Several assigned fragment ions are labeled in the figure inset. Some ions not labeled are assigned as follows: 810 Da, $MH^+$ with loss of $H_2O$; 709 Da, $MH^+$ with loss of Thr and $H_2O$ (or the 716.0 Da ion with loss of $H_2O$); 611 Da, 629 Da ion with loss of $H_2O$; 492 Da, 510 Da ion with loss of $H_2O$; and 458 Da, unassigned.

(sequence 60−62). Table 3 lists the N-terminal sequence data to show that PTH-cystine recovered at sequencing cycle 4 clearly comes from the linkage of Cys62 and Cys77. Figure 5C demonstrates the fragmentation pattern of this peptide during MS-MS. These data clearly indicate that peptide fractions G and H contain two disulfide bonds assigned as Cys44−Cys59 and Cys62−Cys77.

*Thermolysin Digest of Tryptic Peptide Fraction Z.* As described in the previous section (see above), peptide fraction Z contains all disulfides of Cys105 TNFbp except those from domain I (i.e., tryptic peptide fractions C−F in Figure 1) and the first two disulfides of domain II (i.e., tryptic peptide fractions G and H in Figure 1). The peptide fraction was subjected to thermolysin digestion for further cleavage. Figure 6 shows a typical thermolysin peptide map separated by narrowbore C18 reverse-phase HPLC. Sequence determination and mass spectrometric analyses of the isolated peptides were performed, and the obtained data are summarized in Table 4. Peptide Z3 is recovered as a dipeptide

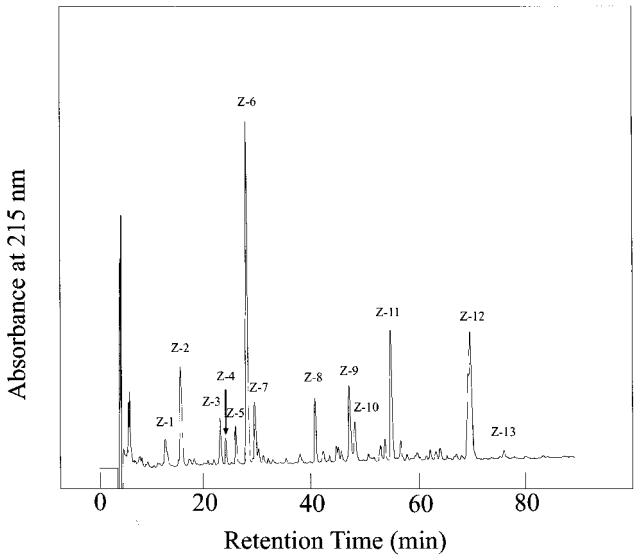


FIGURE 6: Reverse-phase HPLC of tryptic peptide Z following a complete thermolysin digestion in a C18 reverse-phase column (2.1 × 250 mm). Note that in an incomplete digestion, the peak height of peptide Z13 is significantly higher.

Table 4: Structural Characterization of Peptides Obtained from Thermolysin Digestion of Cys105 TNFbp Tryptic Peptide Fraction Z

| peptide fractions | assigned positions | sequence[a] | mass (Da) determined | assignment of disulfide bond(s) |
|---|---|---|---|---|
| Z3 | 94−95 | H-Y | − | |
| Z4 | 65−66 | C-R | | |
| | 84−86 | V-C-G | − | Cys65 to Cys85 |
| Z5 | 143−146 | S-N-C-K | | |
| | 149−151 | L-E-C | − | Cys145 to Cys151 |
| Z6 | 96−99 | W-S-EN | − | |
| Z7 | 143−146 | S-N-C-K | | |
| | 148−151 | S-L-E-C | − | Cys145 to Cys151 |
| Z8 | 108−109 | L-C | | |
| | 125−128 | V-C-T-C | | Cys109 to Cys 126 |
| | 136−139 | E-N-E-C | − | Cys128 to Cys139 |
| Z9 | 65−67 | C-R | | |
| | 84−88 | V-C-G-C-R-K | | Cys65 to Cys85 |
| | 101−103 | F-Q-C | 1334.8(1335.7)[b] | Cys87 to Cys103 |
| Z10 | 65−66 | C-R | | |
| | 84−88 | V-C-G-C-R | | Cys65 to Cys85 |
| | 101−103 | F-Q-C | 1206.5 (1207.6) | Cys87 to Cys103 |
| Z11 | 104−107 | F-C-C-S | | |
| | 116−121 | L-S-C-Q-E-K | | Cys106 to Cys118 |
| | | C | 1282.3 (1283.6) | Cys105 to free Cys |
| Z12 | 140−142 | V-S-C | | |
| | 154−157 | L-C-L-P-Q | 878.1 (879.1) | Cys142 to Cys155 |
| Z13 | 140−147 | V-S-C-S-N-C-K-K | | |
| | 148−151 | S-L-E-C | | Cys142 to Cys155 |
| | 154−157 | L-C-L-P-Q | 1889.6 (1890.1) | Cys145 to Cys151 |

[a] Single-letter standard amino acid codes were used. [b] Masses in parentheses represent the theoretical $MH^+$ species.

in low sequencing yield, while the structure of the other earliest eluting peptides (Z1 and Z2) remains unassigned due to low detection signals in both automated sequencing and mass spectrometry. We speculate that the difficulty in sequencing earlier eluting peptides is due to the smaller molecular size of these peptide fractions. In fact, only two small non-disulfide-linked peptides, peptides Z3 (sequence H-Y) and Z6 (sequence W-S-E-N), were identified. In the remaining disulfide-linked peptides, four peptides, i.e., Z4, Z5, Z7, and Z12, were found to contain only a single disulfide bond. Both sequence and mass spectrometric analyses allow direct assignment of three disulfide bonds,

Cys65−Cys85, Cys145−Cys151, and Cys142−Cys155 (see Table 4). Peptides Z5 and Z7 contain a Cys145−Cys151 bond, and Z12 contains a Cys142−Cys155 bond. These disulfide pairs are near the Cys105 TNFbp C-terminus at domain IV.

Each of the three peptides Z9, Z10, and Z11 contains three sequences possibly linked by two disulfide bonds which can be confirmed by MALDI prompt fragmentation experiments (data no shown). The data indicate that two peptides (sequences of F-Q-C and C-R) are linked to the peptide containing two cysteines (sequence V-C-G-C-R). A similar fragmentation pattern was observed for peptide Z9 as well. We observed that the two disulfides in peptides Z9 and Z10 are equally reactive to TCEP; therefore, it was not possible to isolate partially reduced peptides following partial reduction experiments. The disulfide assignment was then deduced from direct sequence analysis of both peptides Z9 and Z10 (see Table 3 for analysis of peptide Z10). Detection of PTH-cystine at cycles 2 and 4 indicates the pairing of two disulfides, Cys65−Cys85 and Cys87−Cys103.

Peptide Z11, which contains the engineered Cys105 site, contains two disulfide bonds including a possible bond between Cys105 and a cysteine amino acid introduced during refolding. This conclusion is deduced from both N-terminal sequence analysis and measurement of molecular mass (1282.3 Da versus theoretical value of 1283.6 Da). The bond at Cys105 was easily reduced by TCEP and alkylated with the conditions described above, which allowed for the separation of a peptide fraction with two peptides linked by a single disulfide bond, corresponding to sequence 104−107, F-cmC-C-S, and sequence 116−121, L-S-C-Q-E-K. Therefore, the assignment of disulfides for peptide Z11 is Cys106 to Cys119 and Cys105 to a free Cys. The disulfide structure of peptide Z11 was also confirmed by post-source decay fragmentation with CR-MALDI-PSD (data not shown).

The above analyses of peptides from tryptic digestion and from secondary thermolysin digestion of a large tryptic fraction (peptide Z) have identified all 13 disulfide bridges. All disulfide-containing peptides can be generated and isolated through two proteolytic digestions. Following thermolysin digestion of peptide Z, the peptide fractions containing Cys142−Cys155 or Cys142−Cys155 bonds were detected (i.e., peptides Z5, Z7, and Z12). We also searched for a separated peptide peak (i.e., peptide Z13) that contains the last two disulfide bonds. This peptide is not a predominant peptide as shown in Figure 6. However, less extensive thermolysin digestion of tryptic peptide Z generates significantly more peptide Z13. As indicated in Figure 7A, the spectrum of the linear MALDI analysis of peptide Z13 shows a prompt fragmentation pattern. Analysis of the spectrum revealed that there are three peptides linked together by two disulfide bonds. A peptide with a mass of 869 Da was determined to have the sequence 140−147 (V-S-C-S-N-C-K-K). In order to determine the disulfide connectivity of the peptide, it is necessary to fragment the peptide backbone of this peptide between the two cysteine residues before fragmentation of the disulfide bond occurs. We therefore performed CR-MALDI-PSD experiments for this peptide. Figure 7B shows the detection of several fragment ions together with the parent ion. Most ions match the predicted masses derived from cleavage of both peptide bonds and disulfide bridges. The detected fragment ions of 825.6, 940, and 1027 Da correspond to the cleavage sites between

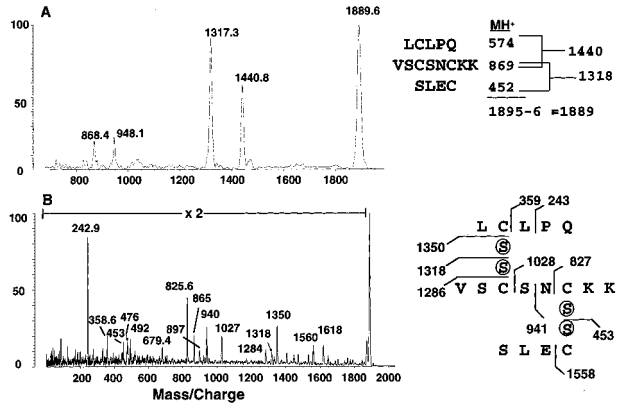


FIGURE 7: MALDI prompt fragmentation and post-source decay MS-MS analysis of peptide Z13 (panels A and B, respectively). The *y* axis indicates the relative ion intensity. The assigned fragments that match the observed fragment ions are indicated at the right side of the panel.

Cys142 and Cys145 (i.e., Cys−Ser, Ser−Asn, and Asn−Cys bonds) prior to the fragmentation of the Cys145−Cys151 bond. It was thus possible to assign the disulfide linkage between residues 145 and 151. In separate experiments, thermolysin digestion of Cys105 TNFbp also allows the isolation of a C-terminal peptide fraction containing only the last two disulfides found in domain IV (data not shown). The isolated peptide was subjected to CR-MALDI-PSD, which produced a fragmentation pattern similar to that of peptide Z13, further indicating a disulfide linkage between Cys145 and Cys151.

*Isolation and Characterization of the C-Terminal Disulfide Structure from CHO Cell-Derived TNFbp.* Glycosylated TNFbp derived from CHO cell expression was partially deglycosylated and subjected to thermolysin digestion. The digest was immediately analyzed by ESI LC-MS to search for C-terminal disulfide-containing peptide. Figure 8A illustrates a chromatogram detected at 215 nm. Fourteen peaks wer obtained at early elution times. However, due to the presence of residual carbohydrates, the thermolysin digestion generates a large glycopeptide fraction eluting as a broader peak at a later retention time (not shown in the chromatogram). This fraction represents protease-resistant core TNFbp structure containing some carbohydrates and most of the disulfide structures. Mass search by LC-MS verified the sequences of more than half of the peptide fractions (see legend for Figure 8A). Only peaks 7 and 14 were identified to contain disulfide-linked fragments. Peak 7 contains two disulfide bonds that link three peptides and is similar to those found in peptide Z8 described in Table 4. Peak 14 has a determined mass of 2099.96 Da by MALDI analysis, and the two sequences, V155-S-C-S-N-C-K-K-S and L160-E-C-T-K-L-C-L-P-Q (numbering is based on the CHO cell-derived TNFbp sequence, see Materials and Methods) were confirmed by N-terminal sequence analysis. This peptide represents the domain IV C-terminal disulfide-containing peptide with two disulfide bonds. This indicates that Cys153 and Cys156 are bound to Cys162 and Cys166, but the exact disulfide arrangement cannot be determined. Both ESI tandem mass spectrometry and CID-MALDI-PSD analyses of the peptide were attempted, but no fragmentation between the disulfides was seen. This peptide was therefore redigested by running it over an immobilized trypsin column and separated by reverse-phase HPLC as seen in Figure 8B. A major peptide fraction at 26.4 min with a mass of 1901.9

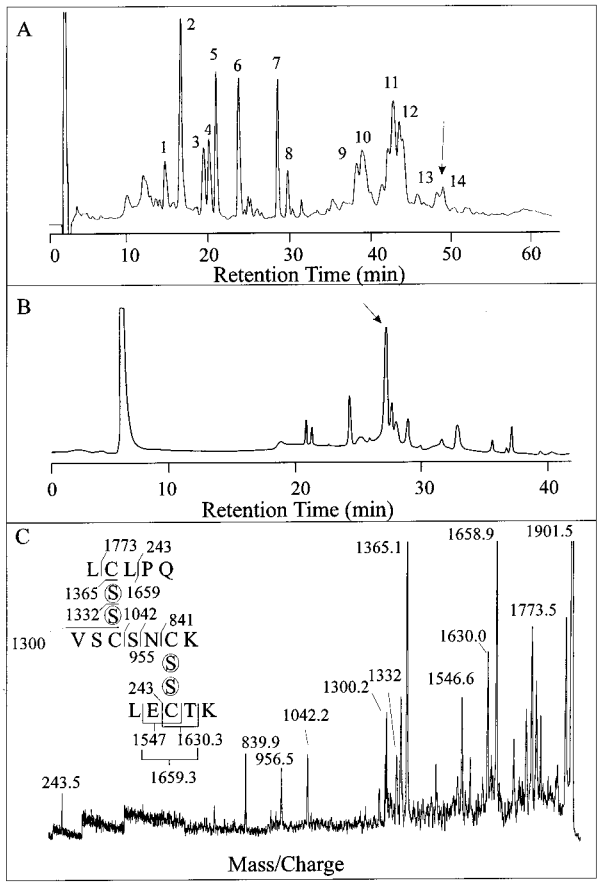


FIGURE 8: Identification of a C-terminal disulfide-containing peptide obtained from CHO cell-derived TNFbp. Panel A: ESI LC-MS analysis of a thermolysin digest showing the chromatographic tracing following 215 nm detection. The identification of peaks recovered are as follows: peak 1, V-K-G-T-E-D-S-G-T-T (sequence 173−182); peak 2 ($MH^+$ = 2578 Da), structure not determined; peak 3, L-G-D-R-E-K-R-D-S (sequence 5−13); peak 4, M-G-Q-V-E (sequence 80−84); peak 5, Phe-Thr-Ala-Ser-Glu-Asn-His (sequence 60−66); peak 7, disulfide-linked fragment containing three sequences, L-C, V-C-T-C-H-A-G; peak 8, Y-W-S-E-N (sequence 106−110); and L-R-E-N-E-C at positions 119−120, 136−142, and 145−150; and peaks 9−13, unidentified mixtures of glycopeptides and peptides. Peak 14 is a C-terminal disulfide-linked peptide fragment containing two sequences: V-S-C-S-N-C-K-K-S (sequence 155−162) and L-E-C-T-K-L-C-L-P-Q (sequence 160−169). Panel B: HPLC separation of the isolated C-terminal disulfide peptide following tryptic digestion detected at 215 nm. A disulfide-containing peptide with a mass of 1901.9 Da is identified in a fraction at 24.6 min. Panel C: post-source decay MS-MS analysis of the isolated disulfide-containing peptide (see panel B).

Da was recovered and proved to contain three sequences, L-E-C-T-K, V-S-C-S-N-C-K, and L-C-L-P-Q, which is structurally similar to peptide Z13 of the *E. coli* TNFbp peptide as described previously. Following CID-MALDI-PSD analysis, as seen in Figure 8C, the mass ions found at 840, 956, and 1042 Da represent those fragmented around the -C-S-N-C- sequence. The overall fragmentation pattern is consistent with the assignment of Cys153−Cys166 and Cys156−Cys162 disulfides. This arrangement is therefore identical to that found in *E. coli* TNFbp as described above.

*Conclusion and Perspectives.* We have performed detailed analysis and searched for strategies to elucidate the complete disulfide structure of *E. coli*-derived TNFbp and to determine the arrangement of two C-terminal disulfide bonds in the fourth domain of CHO cell-derived TNFbp. The first three domains of *E. coli*-derived TNFbp were confirmed to have disulfide structures identical to the TNF-R/NGF-R family cysteine-rich region signature structure. The fourth domain has a different structure than the first three domains where the last four cysteines form two disulfide bonds in opposite positions. A number of approaches employed have led to successful assignment of the TNFbp disulfide bonds, which include generation of disulfide-linked peptides by two proteolytic digestions followed by sequence analysis, partial reduction, and mass spectrometry. Disulfide bonds of some peptides containing either a single or two disulfide(s) can be determined readily by direct sequence analysis via detection of PTH-cystine (*18*, *19*). Samples like peptide E, containing three disulfide bonds, were elucidated by TCEP partial reduction. This indicates that partial reduction can be successfully applied for assigning multiple disulfides in peptides when individual disulfides show differential reactivity to reducing agents. However, partial reduction did not work in several of the TNFbp peptides (data not shown).

MALDI prompt fragmentation can easily assign a single disulfide bond that has linked two cysteine-containing peptides together (25). The method reduces the possible disulfide linkages in peptides containing more than two disulfide bonds as reported by Crimmins et al. (*24*). This technique also proved to be useful in our study for the identification of disulfide linkages of mixed TNFbp peptides. CR-MALDI-PSD or CID-MALDI-PSD can fragment peptides generating fragment ions useful for sequence analysis (*21*). In a negative ion mode, fragmentation at the disulfide bonds occurs as well (*27*). In this report, fragment ions generated by both peptide and disulfide bond fragmentations by PSD were used to determine the disulfide linkages of TNFbp peptides, which could otherwise not be easily elucidated by classical methods. Further description and application using CR-MALDI-PSD in the assignment of complex disulfide peptides will be reported elsewhere (*28*). The analysis of TNFbp complex disulfide structure demonstrated that a variety of strategies are required for a complete identification, yet the mass spectrometric technique as described provides a very sensitive and powerful approach to the application.

In the pH 3.5 X-ray structure of TNFbp, the last two disulfides in domain IV have been shown to have a disulfide linkage pattern that is different from that expected for a disulfide in the cysteine-rich signature structure (*12*). Our chemical identification of the disulfide linkages in TNFbp recombinantly produced in *E. coli* and mammlian cells confirmed that such structure is present in solution and is distinct from other domains. This disulfide arrangement is present at all pH ranges (from pH 3 to 8). The possibility of disulfide rearrangement at high pH needed to be evaluated since the structure near the C-terminal disulfide loop region was disordered in crystal structure and the two last disulfide pairs in domain IV could not be assigned at high pH conditions (*10*). The altered disulfide structure at the fourth domain, which has now been validated over a ranges of pHs, prompted Naismith et al. (*12*) to propose an altered nomenclature for the cysteine-rich region. The biological relevance related to the difference of disulfide arrangement between domain IV and other domains remains unclear and awaits further investigation.

## ACKNOWLEDGMENT

We are grateful to Dr. V. Katta and Mr. D. Chow for their help in training and technical support of the Finnigan MAT ion-trap mass spectrometer.

## REFERENCES

1. Beutler, B. (1992) *The Tumor Necrosis Factors: The Molecules and Their Emerging Roles in Medicine*, Raven Press, New York.
2. Smith, C. A., Davis, T., Anderson, D., Solam, L., Beckmann, M. P., Jerzy, R., Dower, S. K., Cosman, D., and Goodwin, R. G. (1990) *Science 248*, 1019−1023.
3. Loestscher, H., Pan, Y. C., Lahm, H. W., Gentz, R., Brockhaus, M., Tabuchi, H., and Lesslauer, W. (1990) *Cell 61*, 351−359.
4. Schall, T. J., Lewis, M., Koller, K. J., Lee, A., Rice, G. C., Wong, G. H., Gatanaga, T., Granger, G. A., Lentz, R., Raab, H., Kohr, W. J., and Goeddel, D. V. (1990) *Cell 61*, 361−370.
5. Bazan, F. F. (1993) *Curr. Biol. 3*, 603−606.
6. Lapthorn, A. J., Harris, D. C., Littlejohn, A., Lustbader, J. W., Canfield, R. E., Machin, K. J., Morgan, F. J., and Isaacs, N. W. (1994) *Nature 369*, 455−461.
7. Engelmann, H., Novick, D., and Wallach, D. (1990) *J. Biol. Chem. 265*, 1531−1536.
8. Dunn, D. L. (1993) *Am. J. Surg. 166*, 449−455.
9. Feldman, M., Brennan, F. M., and Maini, R. N. (1996) *Annu. Rev. Immunol. 14*, 397−440.
10. Banner, D. W., D'Arcy, A., Janes, W., Gentz, R., Schoenfeld, H. J., Broger, C., Loetscher, H., and Lesslauer, W. (1993) *Cell 73*, 431−445.
11. Naismith, J. H., Devine, T. Q., Brandhuber, B. J., and Sprang, S. R. (1995) *J. Biol. Chem. 270*, 13303−13307.
12. Naismith, J. H., Devine, T. Q., Kohno, T., and Sprang, S. R. (1996) *Structure 4*, 1251−1262.
13. Boone, T. C., Chazin, V., Keney, W., Swanson, E., and Altrock, B. (1987) *Dev. Biol. Stand. 69*, 157−168.
14. Rodseth, L. E., Brandhuber, B., Devine, T. Q., Eck, M. J., Hale, K., Naismith, J. H., and Sprang, S. R. (1994) *J. Mol. Biol. 239*, 3321−3335.
15. Hale, K. K., Smith, C. G., Vanderslice, R. W., Baker, S., Russel, D. A., Rivera, R. I., Dripps, D., and Kohno, H. (1991) *J. Cell Biochem. 15F*, 113.
16. Lu, H. S., Clogston, C. L., Wypych, J., Parker, V. P., Lee, T. D., Swiderek, K., Balterea, R., Patel, A. C., Chang, D. C., Brankow, D. W., Liu, X.-D., Ogden, S. G., Karkare, S. B., Hu, S. S., Zsebo, K. M., and Langley, K. E. (1992) *Arch. Biochem. Biophys. 298*, 150−158.
17. Gray, W. R. (1993) *Protein Sci. 2*, 1732−1748.
18. Hara, S., Liu, N., Meng, S.-Y., and Lu, H. S. (1996) *Biochim. Biophys. Acta 1292*, 168−176.
19. Haniu, M., Hsieh, P., Rohde, M. F., and Kenney, W. C. (1994) *Arch. Biochem. Biophys. 310*, 433−439.
20. Cornish, T. J., and Cotter, R. J. (1994) *Rapid Commun. Mass Spectrom. 8*, 781−785.
21. Cordera, M. M., Cornish, T. J., Cotter, R. J., and Lys, I. A. (1995) *Rapid Commun. Mass Spectrom. 9*, 1356−1361.
22. Jonscher, K. R., and Yates, J. R. (1997) *Anal. Biochem. 244*, 1−15.
23. Schwartz, J. C., and Jardine, I. (1996) *Methods Enzymol. 270*, 552−587.
24. Crimmins, D. L., Saylor, M., Rush, J., and Thoma, R. S. (1995) *Anal. Biochem.*, 355−361.
25. Patterson, S. D., and Katta, V. (1994) *Anal. Chem. 66*, 3727−3732.
26. Jones, M. D., Merewether, L. A., Clogston, C. L., and Lu, H. S. (1994) *Anal. Biochem. 215*, 135−146.
27. Zhou, J., Ens, W., Poppe-Schriemer, N., Standing, K. G., and Westmore, J. B. (1993) In *J. Mass Spectrom. Ion Processes 126*, 115−122.
28. Jones, M. D., Patterson, S. D., and Lu, H. S. (1998) *Anal. Chem.* (in press).

BI971696K